

A formal methodology for avoiding hyperstaticity when connecting an exoskeleton to a human member

Nathanaël Jarrassé
Guillaume Morel

Université P. et M. Curie Paris VI, ISIR (Institut des Systèmes Intelligents et de Robotique) CNRS - UMR 7222
4 place Jussieu, 75005 Paris - France
Telephone: +33.1.44.27.51.41
Emails : jarrasse@isir.fr, guillaume.morel@upmc.fr

Abstract—The design of a robotic exoskeleton often focuses on replicating the kinematics of the human limb that it is connected to. However, human joint kinematics is so complex that in practice, the kinematics of artificial exoskeletons fails to reproduce it exactly. This discrepancy results in hyperstaticity. Namely, uncontrolled interaction forces appear.

In this paper, we investigate the problem of connecting an exoskeleton to a human member while avoiding hyperstaticity; to do so, we propose to add passive mechanisms at each connection point. We thus introduce a formal methodology for avoiding hyperstaticity when connecting wearable robotic structures to the human body.

First, analyzing the twist spaces generated by these fixation passive mechanisms, we provide necessary and sufficient conditions for a given *global isostaticity condition* to be respected. Then, we derive conditions on the number of Degrees of Freedom (DoFs) to be freed at the different fixations, under full kinematic rank assumption. We finally apply the general methodology to the particular case of a 4 DoF shoulder-elbow exoskeleton. Experimental results allow to show an improvement in transparency brought by the passive mechanism fixations.

I. INTRODUCTION

Whatever the particular use they are designed for (augmenting human force capabilities, helping a patient during neurophysical rehabilitation, haptic or master device, etc.), the major purpose of exoskeletons is to transmit forces to the connected human limb. Designing these physically connected devices faces a rather challenging set of constraints: adaptability to kinematics variations between human subjects is required; large force capability is desirable over a large workspace; simultaneously transparency (i.e. capability of applying minimal forces in resistance to the subject's movements) is of high importance. Designing the kinematics of an exoskeleton consists of trying to replicate the human limb kinematics. This brings a number of advantages: similarity of the workspaces, singularity avoidance [1], natural feeling of the connection with human subject. If the kinematics of the human limb and the exoskeleton are the same, there is a one-to-one mapping between the joint torques exerted by the robot and the joint torques applied to the human subject, whatever

the joint configuration. A major drawback of the exoskeleton paradigm is that, in fact, human kinematics is impossible to replicate with a robot. Two problems occur: morphology drastically varies by the subject and, for a given subject, the joints kinematics is very complex and cannot be imitated by conventional robot joints [2]. In fact, it is impossible to find any consensual model of the human kinematics in the biomechanics literature due to complex geometry of bones interacting surfaces. For example, different models are used for the shoulder-scapula-clavicle group[3].

Since human limb models are only approximations, exoskeletons are imperfect. This generates kinematic compatibility problems. Indeed, when connecting two-by-two the links of two *kinematically similar* chains that are not perfectly identical, hyperstaticity occurs. This phenomenon leads, if rigid models are used, to the impossibility of moving and the appearance of non-controllable (possibly infinite) internal forces. In practice, though, rigidity is not infinite and mobility can be obtained thanks to deformations. When a robotic exoskeleton and a human limb are connected, most likely, these deformations occur at the interface between the two kinematic chains, caused by the low stiffness of skin, tissues. Solutions found in the literature to cope with problem are of two kinds. In a first approach the exoskeleton design can be thought in such a way that adaptation to human limb kinematic is maximized. Robotic segments with adjustable length were thus developed, and pneumatic systems were added to introduce elasticity in the robot fixations and adaptability to variant limb section [4]. All these approaches add to the exoskeleton complexity while they are not formally proven to solve the hyperstaticity problem.

The second approach is different and consists in adding passive DoF to the structure. Some researchers works at a primary level, designing passive articulated lockable mechanisms able to align the robot axis on the human one during the first initial movements of the comanipulation session [5]. The last and simple solution of this approach consists of keeping the exoskeleton structure unchanged, but adding passive DoF at

the connections between the robot and the limb [6] to limit undesired forces appearance. Indeed, it is a general concept in theory of mechanisms for years that adding passive DoF is a way of releasing the degree of hyperstaticity ([7], [8]). No quantification is shown, only simple model that can't be used during the design process.

Rather, thanks to basic theory of mechanisms, we consider in this paper a generic problem of coupling an exoskeleton with a human limb by adding passive DoF at the interface between the structures and derive a formally proved set of conditions (Section I) allowing us to solve the problem of morphology compatibility, misalignment errors but also force transmission by removing hyperstaticity. In Section II, the method is applied to ABLE, a 4 active DoF arm exoskeleton. In Section III, the experimental setup for the fixation evaluation is described and finally in Section IV, results of preliminary evaluation of these isostatic fixations are presented and discussed.

II. GENERAL METHODOLOGY

The main question addressed in this paper is: given a proposed exoskeleton structure designed to (approximately) replicate a human limb kinematic model, how to connect it to the human limb while avoiding the appearance of uncontrollable forces at the interface? The answer takes the form of a set of passive frictionless mechanisms used to connect the robot and the subject's limb that allows to avoid hyperstaticity.

A. Problem formulation

We consider two different serial chains with multiple couplings as illustrated in Fig. 1. One represents a human limb \mathbf{H} and the other the robot structure \mathbf{R} .

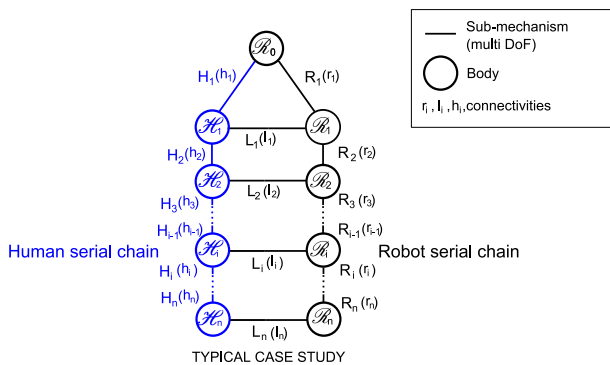


Fig. 1. Schematic of two serial chains parallel coupling

The base body of the exoskeleton is supposed to be attached to a body of the human subject. This common body is denoted $\mathcal{R}_0 \equiv \mathcal{H}_0$. The robot and the limbs are supposed to be connected through n fixations. Each fixation is a mechanism \mathbf{L}_i for $i \in \{1, \dots, n\}$ consisting in a passive kinematic chain which connects a human body \mathcal{H}_i to a robot body \mathcal{R}_i . Mechanisms \mathbf{L}_i are supposed to possess a connectivity l_i . Recall that connectivity is the minimum and necessary number of joint scalar variables that determine the geometric configuration of the \mathbf{L}_i chain [9]. Typically, \mathbf{L}_i will be a nonsingular serial

combination of l_i one DoF joints. The fixation can be an embedment ($l_i = 0$) or can release several DoFs, such that:

$$\forall i \in \{1, \dots, n\}, \quad 0 \leq l_i \leq 5 \quad . \quad (1)$$

Indeed choosing $l_i \geq 6$ would correspond to complete freedom between \mathcal{H}_i and \mathcal{R}_i which would not make any practical sense in the considered application where force transmission is required.

Between \mathcal{R}_{i-1} and \mathcal{R}_i , on the robot side, there is an active mechanism \mathbf{R}_i which connectivity is denoted r_i . Similarly, between \mathcal{H}_{i-1} and \mathcal{H}_i on the human side, there is a mechanism \mathbf{H}_i of connectivity h_i . Note that, due to the complexity of human kinematic h_i is not always exactly known, and literature from biomechanics provides controversial data on this point. For example, the elbow is often modeled as a one DoF joint, but in reality a residual second DoF can be observed [10].

Our goal is to design mechanisms \mathbf{L}_i with $i \in \{1, \dots, n\}$ in such a way that on one side, all the forces generated by the exoskeleton on the human limb are controllable and on the other side, there is no possible motion for the exoskeleton when the human limb is still. We shall thus consider in the next that the human limbs are virtually attached to the base body \mathcal{R}_0 . This represents the case, when the subject does not move at all. The resulting overall mechanism, depicted in Fig. 2, is denoted \mathbf{S}_n .

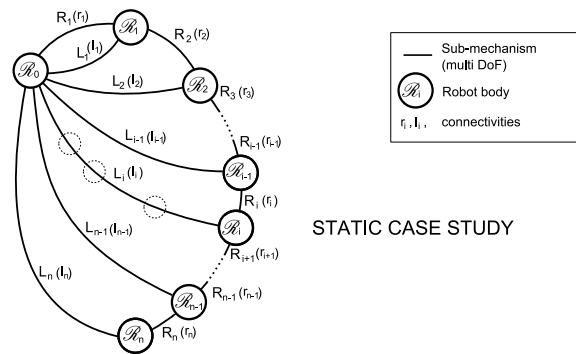


Fig. 2. Studied problem with a fixed human limb

A proper design for the passive mechanisms \mathbf{L}_i shall guarantee that, in the absence of any external forces, both:

$$\forall i \in 1 \dots n, \quad \mathbf{S}^n T_i = \{0\} \quad \text{and} \quad (2a)$$

$$\forall i \in 1 \dots n, \quad \mathbf{S}^n W_{i \rightarrow 0} = \{0\} \quad , \quad (2b)$$

where $\mathbf{S}^n T_i$ is the space of twists describing the velocities of robot body \mathcal{R}_i relative to \mathcal{R}_0 when the whole mechanism \mathbf{S}_n is considered and $\mathbf{S}^n W_{i \rightarrow 0}$ is the space of wrenches (forces and moments) statically admissible transmitted through the \mathbf{L}_i chain on the reference body \mathcal{R}_0 (the blocked arm), i.e. the space of the forces (forces and moments) resulting from a possible hyperstatism appearing when the whole mechanism \mathbf{S}_n is considered.

Equation (2a) expresses the fact that the mobility of any robot body connected to a human limb should be null, which is required since the human member is supposed here to be

still. Moreover, Eq. (2b) imposes that, considering the whole mechanism, there can be no forces of any kind exerted on the human limb. Indeed, since the actuators are supposed to apply a null generalized force, the presence of any force at the connection ports would be an uncontrollable force due to hyperstaticity.

Therefore, Eq. (2) is referred in the next as *global isostaticity condition*.

B. Conditions on the twist space ranks

At first, one can notice the recursive structure of the considered system: if we name \mathbf{S}_i the sub-mechanism constituted by the bodies \mathcal{R}_0 to \mathcal{R}_i and the chains \mathbf{R}_0 to \mathbf{R}_i and \mathbf{L}_0 to \mathbf{L}_i , we can represent \mathbf{S}_i recursively from \mathbf{S}_{i-1} , as in Fig. 3, where m_{i-1}

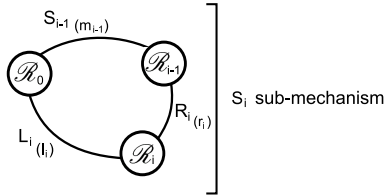


Fig. 3. Recursive structure \mathbf{S}_i of the system

is the connectivity of \mathbf{S}_{i-1} . In this convention, \mathbf{S}_0 represents a zero DoF mechanism. Using this recursive representation of the studied mechanism \mathbf{S}_n one can establish the following proposition:

Proposition 1: The conditions (2) are equivalent to :

$$\forall i \in 1 \cdots n, \quad \dim(T_{\mathbf{S}_{i-1}} + T_{\mathbf{R}_i} + T_{\mathbf{L}_i}) = 6 \quad \text{and} \quad (3a)$$

$$\forall i \in 1 \cdots n, \quad \dim(T_{\mathbf{S}_{i-1}} \cap T_{\mathbf{R}_i}) = 0 \quad \text{and} \quad (3b)$$

$$\dim(T_{\mathbf{S}_n}) = 0 \quad , \quad (3c)$$

where $T_{\mathbf{S}_j} = \mathbf{S}_j T_j$ is the space of twists describing the velocities of \mathcal{R}_j relative to \mathcal{R}_0 , when \mathbf{S}_j is considered isolated from the rest of the mechanism (then it is different from $\mathbf{S}_n T_j$), $T_{\mathbf{R}_i}$ is the space of twists produced by \mathbf{R}_i - i.e. the space of twists of \mathcal{R}_i relative to \mathcal{R}_{i-1} if they were only connected through \mathbf{R}_i , $T_{\mathbf{L}_i}$ is the space of twists produced by \mathbf{L}_i i.e. the space of twists of \mathcal{R}_i relative to \mathcal{R}_0 if they were only connected through \mathbf{L}_i . ■

The demonstration can be found in the appendix.

Remarkably, conditions (3) involve the space of twists generated by \mathbf{R}_i and \mathbf{L}_i when taken isolated, which is of great help for design purposes. In the next, we convert these conditions into constraints on the connectivities $r_i = \dim(T_{\mathbf{R}_i})$ and $l_i = \dim(T_{\mathbf{L}_i})$. To do so, we suppose that kinematic singularities are avoided. In other words, summing the subspaces of twists will always lead to a subspace of maximum dimension given the dimensions of individual summed subspaces. This hypothesis will lead to determine how many DoFs shall be included in the passive fixation mechanisms \mathbf{L}_i . Of course as it is usual in mechanism design, when a particular design is finally proposed, it will be necessary to verify *a posteriori* the singularity avoidance condition.

C. Conditions on connectivities

At first, let's compute the connectivity of \mathbf{S}_i . One has:

$$(3a) \Rightarrow \forall i \in 1 \cdots n, \quad m_{i-1} + r_i + l_i \geq 6 \quad (4)$$

with $m_i = \dim(T_{\mathbf{S}_i})$. This condition comes directly from the fact that, from any vector subspaces \mathbf{A}, \mathbf{B} and \mathbf{C} of a vector space \mathbf{E} , $\dim(\mathbf{A} + \mathbf{B} + \mathbf{C}) \leq \dim(\mathbf{A}) + \dim(\mathbf{B}) + \dim(\mathbf{C})$.

Secondly:

$$(3b) \Rightarrow \forall i \in 1 \cdots n, \quad m_{i-1} + r_i \leq 6 \quad (5)$$

This condition comes from the fact that if \mathbf{A} and \mathbf{B} are two vector subspaces of \mathbf{E} and $\dim(\mathbf{A}) + \dim(\mathbf{B}) > \dim(\mathbf{E})$, then $\mathbf{A} \cap \mathbf{B} \neq \{0\}$.

Finally:

$$(3c) \Rightarrow m_n = 0 \quad (6)$$

At this stage, it is important to notice that Eq. (4,5,6) express only necessary conditions on l_i , m_i and r_i . These conditions are not sufficient since any particular configuration of the axes that would decrease the rank of any kinematic equation for \mathbf{S}_n would change the dimension of the combined space of twists. We will assume, in the next, that such singularities are avoided, which is of course to be verified a posteriori when considering a particular design.

This assumption allows to derive a relationship m_i and l_i and r_i . One has:

$$T_{\mathbf{S}_i} = T_{\mathbf{L}_i} \cap (T_{\mathbf{R}_i} + T_{\mathbf{S}_{i-1}}) \quad (7)$$

This last equation directly results from the space sum law for serial chains and the intersection law for parallel chains (see [11]). Furthermore, since for any vector subspace subspaces \mathbf{A} and \mathbf{B} , $\dim(\mathbf{A}) + \dim(\mathbf{B}) = \dim(\mathbf{A} + \mathbf{B}) + \dim(\mathbf{A} \cap \mathbf{B})$, one gets:

$$\begin{aligned} m_i &= \dim(T_{\mathbf{L}_i}) + \dim(T_{\mathbf{R}_i} + T_{\mathbf{S}_{i-1}}) - \dim(T_{\mathbf{L}_i} + T_{\mathbf{R}_i} + T_{\mathbf{S}_{i-1}}) \\ &= \dim(T_{\mathbf{L}_i}) + \dim(T_{\mathbf{R}_i}) + \dim(T_{\mathbf{S}_{i-1}}) - \dim(T_{\mathbf{R}_i} \cap T_{\mathbf{S}_{i-1}}) \\ &\quad - \dim(T_{\mathbf{L}_i} + T_{\mathbf{R}_i} + T_{\mathbf{S}_{i-1}}) \\ &= l_i + r_i + m_{i-1} - 6 \end{aligned}$$

Since $m_0 = 0$, this recursive equation simplifies to:

$$m_i = \sum_{j=1}^i (l_j + r_j) - 6.i \quad (8)$$

The conditions (4),(5) and (6) can thus be written as

$$\forall i \in 1 \cdots n, \quad \sum_{j=1}^i (l_j + r_j) \geq 6.i \quad (9a)$$

$$\forall i \in 1 \cdots n, \quad \sum_{j=1}^{i-1} (l_j + r_j) + r_i \leq 6.i \quad (9b)$$

$$\sum_{j=1}^n (l_j + r_j) = 6.n \quad (9c)$$

Global isostaticity will be reached if we are able to find axis configurations preventing from the appearance of geometrical particularities (that will badly impact the kinematic equations

system rank) for the L_j chain that verify the three conditions (9).

One can notice that (9c) points out the total number of l_j for the S_n mechanism, while (9a) gives the minimal value (to prevent from hyperstaticity in the sub-mechanisms S_j) for L_j and (9b) provides the maximal one (to prevent from internal mobility in the S_j).

Thanks to these last equations, we are able to calculate the different possible solutions for distributing the additional passive DoF at fixations over the structure:

- the possible choices for l_1 are such that $5 \geq l_1 \geq 6 - r_1$.
- for each choice of l_1 , the possible choices for l_2 are such that $5 \geq l_2 \geq 12 - r_1 - r_2 - l_1$.

This leads to a tree that groups all the admissible combinations for l_i , as illustrated in Fig (4).

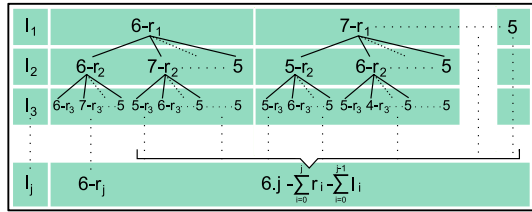


Fig. 4. Tree of possible solutions for the number of passive DoFs to add at every fixation point

Out of this tree, many solutions are feasible from the point of view of mechanism theory but are not adequate for a correct transmission from an exoskeleton to a human member. Generally speaking, an important aspect to be considered is the force transmission: through any linear or rotational DoF that is not freed by the fixation mechanism, a force or a moment will be transmitted to the human limb, which is surrounded by soft tissues. Therefore, typically, transmitting moments around P_i would lead to locally deform the tissues which in turn can generate discomfort. The next section illustrates, on a concrete spatial example involving two fixations, how to integrate this kind of considerations in the design of fixation mechanisms.

III. APPLICATION TO A GIVEN EXOSKELETON

A. ABLE: an upper limb exoskeleton for rehabilitation

ABLE (see Figure 5) is a 4 axis exoskeleton that has been designed by CEA-LIST on the basis of an innovative actuation technology ([12]). Its kinematics is composed of



Fig. 5. ABLE 4 axis exoskeleton actuated by screw-and-cable actuators

a shoulder spherical arrangement made with 3 coincident

axes and a 1 DoF pivot elbow. The forearm, terminated by a handle, is not actuated. Its kinematics is sketched in Figure 6. Most of the technological originality of ABLE comes from

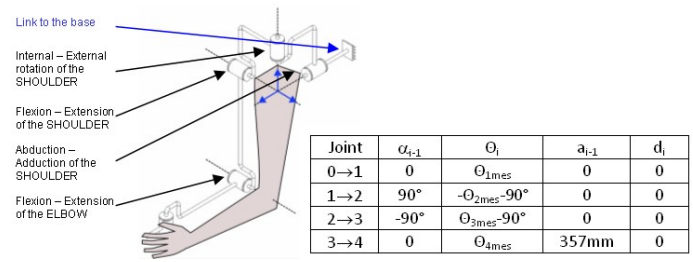


Fig. 6. Kinematics of ABLE

its actuation and transmission system, which is based on a patented Screw-and-Cable system (SCS) [13]. The hardware characteristic of ABLE makes it an excellent platform for physical rehabilitation therapies. Its low joint stiffness and naturally compliant joints ensure the safety when using the robot for patients with physical disability. Unfortunately, first experiments shows us that without paying attention to the fixations by simply connecting upper arm and forearm middle areas to the orthosis using medical straps, which induce hyperstaticity, an alteration of natural movements appears [14]. This alteration is mainly due to a lack of synchronization between the arm joints: synergies seem to be perturbed even with an great transparency (low inertia and friction phenomenons).

B. Fixations design for ABLE

In this section, we apply general method proposed in Sec. II to ABLE. Firstly, since ABLE comprises an upper arm and

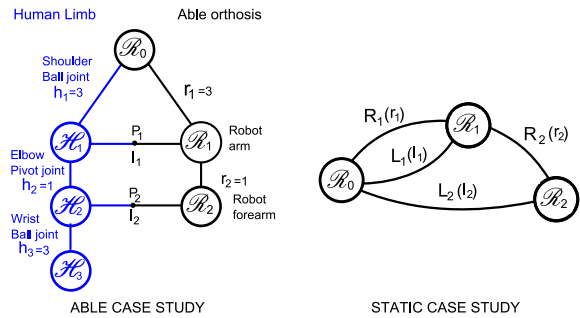


Fig. 7. Schematic of the ABLE and human arm coupling

a forearm, we choose to use two fixations, one for each arm body (See Fig 7). The total number of passive DoF to be added is given by (equ. (9c)):

$$\sum_{j=1}^{n-2} l_j = 12 - \sum_{j=1}^{n-2} r_j = 12 - (3 + 1) \Rightarrow l_1 + l_2 = 8 \quad (10)$$

Moreover, for the first fixation, the hyperstaticity avoidance constraint is (equ. (9a) and (9b)):

$$6 - r_1 \leq l_1 \leq 6 \Rightarrow 3 \leq l_1 \leq 5 .$$

In the case of only two fixations, since the total number of DoFs is fixed, the tree of possible solutions consists of parallel branches where l_1 is chosen between 3 and 5 and $l_2 = 8 - l_1$, which gives three couples for (l_1, l_2) : (3,5), (4,4) and (5,3). It can be verified that these three couples verify the constraints. The derivation of the complete catalog of all possible arrangements among the three proposed distributions for the passive DoFs does not fit in the format of the paper. We here focus on three possible solutions that are represented in Figure 8.

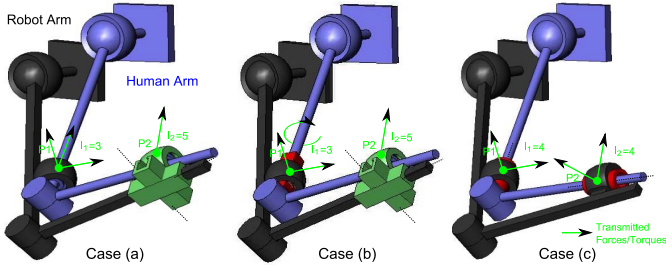


Fig. 8. Schematic of possibilities for coupling ABLE to an human arm. Case (a): ball joint alone at P_1 and ball joint on 2 slides at P_2 ; case (b): Universal joint + 1 slide (in red) at P_1 and ball joint on 2 slides at P_2 ; case (c) Ball joints with slides (in red) at both P_1 and P_2 .

The solutions (a) and (b) correspond to $(l_1 = 3)$ and $(l_2 = 5)$. This choice is somehow intuitive, because we have $l_i = 6 - r_i$ for $i = 1, 2$, which means that each subsystem S_i is independently chosen to be isostatic, resulting in a globally isostatic system. However, Solution (a) shall be rejected because the selected freed DoF (a ball joint at the fixation point P_1) leads to a lack of rank for the closed chain equations. Indeed, there is a possible internal motion that is a rotation around the axis joining P_1 to the center of rotation of the robot shoulder. Rather, Solution (b), which uses for the freed DoF at P_1 two rotations perpendicular to the upper arm axis and one translation along the upper arm axis should be used. Indeed, it can be verified that for case (b) the closed loop kinematic equations for both S_1 and S_2 are of full rank.

However, for the practical realization, Solution (c) was kept. This solution involves $l_1 = l_2 = 4$ freed DoFs. It is less intuitive than the previous choice because S_1 , taken alone, is a loop with $l_1 + r_1 = 7$ kinematic constraints, therefore the robot arm \mathbf{B}_1 connected through \mathbf{L}_1 to \mathbf{H}_1 has one degree of freedom even if \mathbf{H}_1 is unmoving. However, when the whole system is considered, there is no mobility for the exoskeleton if the human arm is kept still.

Solution (c) has the following advantage over solution (b): with solution (c), generating a moment to the human upper arm around its axis (D) is obtained by applying opposite pure forces perpendicular to (D) at points P_1 and P_2 ; rather, with solution (b), it is directly transmitted to the upper arm through the fixation \mathbf{L}_1 (transmissible moment at P_1 around (D)). This is illustrated in Fig. 9. Applying directly this moment through a tight fixation is in fact a transmission by friction that can generate high tangential forces on the skin, and thus, pain. Note that the solution sketched in Fig. 9 is not possible at full extension, where the two segment axes are aligned. In this

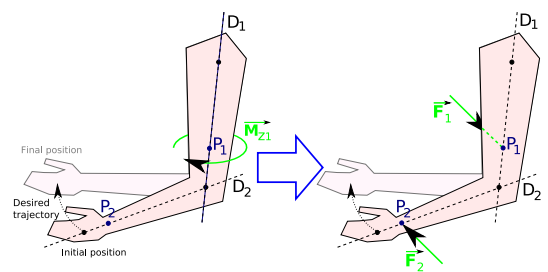


Fig. 9. Transmitting a moment around the upper arm axis with solution (b) (left) and (c) (right)

case, the singular avoidance condition is not verified. This is not a problem in practice because ABLE is equipped with a range limit a few degrees before full extension. More informations and rules on how to choose appropriate DOFs for the fixation mechanisms can be founded in [15].

C. Fixations realization

To free three rotations and a translation at every fixation point, we use a ball joint mounted on a slide. We have

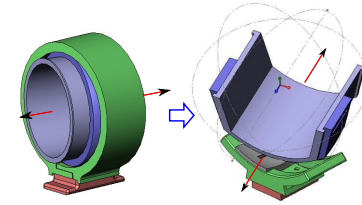


Fig. 10. Fixation simplification and realization

transformed the standard ball-joint into a reduced (but fully functional) ball-joint mechanism allowing the subject arm not to be fully surrounded, which eases the installation and increases the freedom sensation. We have also placed the slide after the ball-joint mechanism in the kinematic chain, in such a way that the direction where no force can be transmitted is always the main direction of the human limb, no matter the amount of discrepancy appearing between ABLE links dimension and the subject arm dimensions. Two of these isostatic fixations were built in ABS with a rapid prototyping machine and the use of low profile linear guides (for the translation DoF). Because of that building process, added weight and cost are negligible (150 g per fixation or less than 3% of the mobile parts effective weight, and cost of fabrication is approx. 0.3% of the exoskeleton parts cost). They were both fitted with one force sensor between the base and the 4 joints (ATI Nano43 6-axis Force/Torque sensor) allowing us to reconstruct the 3 forces and 3 torques components at P_1 and P_2 respectively).

For these experiments, the fixations were also equipped with a removable metallic pin through all the fixation, allowing us to quickly lock the passive DoF without detaching the subject from the exoskeleton. This lock allows us to obtain a classical fixation with no passive DoF and to compare the behavior of a subject attached to ABLE with or without fixations. These

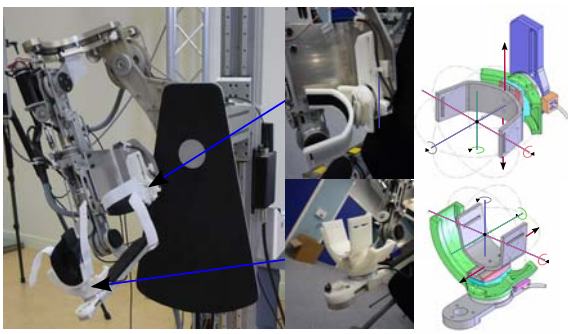


Fig. 11. The two fixations on the exoskeleton

fixations were mounted on the 4 DoF ABLE exoskeleton at specific positions:

- The arm fixation is placed near the elbow, just under the triceps, in an area where the arm section do not vary too much during the elbow flexion/extension.
- The forearm fixation is placed near the wrist for the same reasons, and because the forearm section at this place is not round and allow to block the forearm to force the use of the fixation prono-supination DoF without firmly strapping the tissues.

The possible motions left by the passive fixations have the following ranges:

DoF	Arm Fixation	Forearm Fixation
Rotation1	60°	120°
Rotation2	20°	20°
Rotation3	360°	360°
Translation	20mm	20mm

IV. EXPERIMENTAL EVALUATIONS

An experimental protocol was tested to quantify the hyperstatic forces level reached during a comanipulation of an arm inside a robotic exoskeleton. At the same time, the interaction improvement that such isostatic fixations can allow will be studied.

Healthy people were so asked to perform particular movements with their arm connected to the ABLE exoskeleton through the previously designed fixations. Exchanged force level at the interfaces were recorded, allowing us a transparency level quantification.

A. Control

We need to make the ABLE exoskeleton the more transparent we can, in order to quantify the force level due to hyperstaticity alone. Compensations were thus deployed on the robot, for the subject to perform natural unperturbed movements. The robot controller architecture is based on a PC104 board with two endowed 3 channel axis controller. It runs at 1kHz the control law thanks to a real time operating system (RTlinux). As the ABLE exoskeleton is only fitted with optical encoders, we do not have access to an acceleration signal. The transparency is thus achieved by an experimentally identified

gravity compensation for all axis and also by compensating for the residual dynamic dry friction compensation. This residual friction compensation has been developed in order to blend the friction phenomenons on all axis, and so on not to lead subject to do non-natural moves because of the feelings differences between every joints. Another controller based on a PC104 board with two Analog and Digital I/O PCI card (Sensory 526) is used for acquiring the readings of the F/T sensors during the exercise every 5ms (RTAI real time operating system).

B. Experimental setup

During all the experiments, we assume the exoskeleton to be "transparent" due to the gravity and friction compensation. Analyzing the interaction force and torque variations at the interfaces during the same movement with isostatic fixations and without (locked case) will allow us to evaluate their impact on preventing for the appearance of uncontrolled forces (and thus on the general transparency level) but also to quantify them roughly.

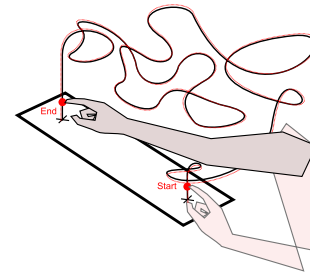


Fig. 12. Complex 3D following task

The subject is asked to follow a metallic wire (in a workspace about 60cm long, 20 cm deep and 20 cm high) with a complex shape with a metallic stem from one end to another and inversely. The system is "electrified" so that the subject is told by a sound when the contact between the wire and the stem is lost. This exercise allows to study the impact of the passive DoF fixations on general moves because it needs the subject to use all his arm joints to be completed (elbow extension during the move vary approximately from 15 deg. to 105 deg; 0 denoting full extension). The end area was positioned in such a way to be reachable by the subject when performing a full elbow extension.

Before recording the trajectory and force data, the subject is asked to perform the exercise several times in order to discover how to use the exoskeleton and not to observe learning phenomenon during the recorded three movements repetition.

V. RESULTS AND DISCUSSIONS

This protocol was evaluated on 18 healthy naive subjects. Principal results are presented below. In Figure 13, we plotted the force and torque norm mean during the experiments, for the two sensors, averaged across the eighteen subjects (the torque is computed at the rotation center of the fixation). We can observe a decrease in the interaction force level by

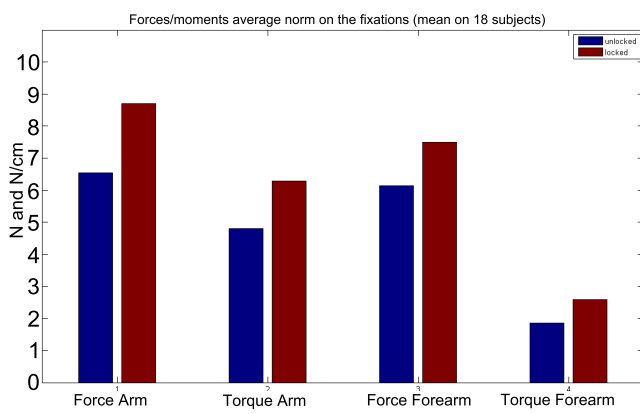


Fig. 13. Forces/torques average norm on the fixations (mean on 18 subjects) Blue unlocked and red locked

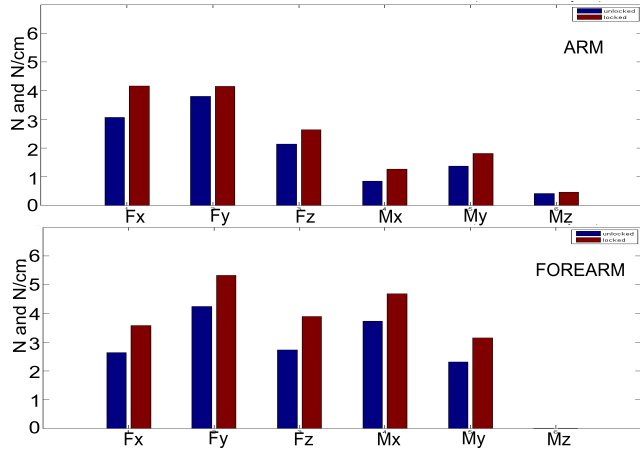


Fig. 14. Mean of each force and moment absolute value for the two sensors. Blue unlocked and red locked

25% for the arm fixation and by 20% for the forearm. If we observe the mean of each force and moment absolute value for the sensors (Figure 14), we can more precisely analyze the phenomena. One particular phenomenon is the arm torques measured around the Z axis that seems to stay at a very low level during the experiments. These reduced decreases of some components can be linked with a phenomenon observed during these experiments: a push-pull effect between the parts because of the usury of the plastic material. We cannot quantify this phenomenon impact, but it has surely lead to decrease the performance of these fixations.

Although these preliminary mixed results appears promising, we realize that the task was too endpoint oriented to force the subject to perform the same trajectory (same speed and path) during the two experimental stages. Only the start and end areas are really constrained, so the subject can transform or adapt -even unconsciously- his arm trajectory. This path alteration thus limits our comparison between the two fixations modes.

A. Discussions

Our preliminary and simple fixations, even mechanically limited, helped to reduce the hyperstatic uncontrolled and undesired interaction force level up to 25 per cent in comparison with classic rigid fixations. But what is really important is that our approach seems to be consistent.

Beside the release of DoF along the human limb advocated by several researcher teams, it is really the hyperstaticity phenomena we studied that is targeted: indeed, we achieve to even more reduce the interaction force level by also releasing the rotation DoF. And that proves that reaching isostaticity in the coupling can improve interaction.

This method allows to design fixations that preserve human mobility. These fixations, if they were perfectly isostatic and without friction (and that gravity and friction compensation were ideally perfect), will lead to the disappearance of some force and torque components (Fx, Mx, My and Mz in our case), only allowing the transmission of the desired force components on the ABLE exoskeleton case. Alas, in our experiment, even if the level of the 4 other interaction forces/torques is reduced (see Fig. 13), it stay still important even with the passive added DoF. Even if it is very difficult to ask subjects to perform the same joint trajectory with a varying robotic configuration, several other explanations can be formulated to explain the system performance limitations:

- the plastic realization of the fixation,
- the limited workspace of the passive DoF (notably for the translation),
- the appearance of uncontrolled and undesired contact points (between the robot and the human limbs) during the movement, leading to a partial read of the exchanged force level on the F/T sensors

Theses hypothesis will be verified in future thanks to new experiments we are conducting with more subject and some statistical analysis with error analysis. This campaign is being performed with metal made fixations and a innovative mechanisms that limits the frictions phenomenons. We are confident in a performance increase after having notice the deformations and the frictions of our rapidprototyping made fixations.

Beside these quantitative results, all the subjects mentioned they feel more comfortable with the passive DoF released. An interesting extension of these evaluations should be performed in the future to fit the subject with motion capture sensors and record the task movement with the robot (and the two fixations states) and without. Comparing the trajectory realized by the free arm to the ones followed when connected to the robot could help to quantitatively describe the benefits of isostatic fixations in the "task space" rather than in the "force space": balancing the forces data with a coefficeint describing the path variation with and without the fixations released could help to obtain realistic results.

VI. CONCLUSION

In this paper we presented a methodology aimed at designing the kinematics of fixations between an exoskeleton and

a human member. The provided solution avoids hyperstaticity but also adapts to large variations on the human limb geometry without requiring a complex adaptable robot structure. Thanks to this method, we prototyped isostatic fixations for a 4 DoF exoskeleton and experimentally verified their benefit on minimizing uncontrollable hyperstatic forces at the human robot interface.

These first results show that hyperstatic constraints lead to not negligible uncontrolled force appearance at the interface. This is consistent with the Schiele preliminary experiments [6].

Interestingly, the addition of passive degrees of freedom can be done through light, compact and unexpensive mechanisms. In the case of ABLE, it is estimated that the passive mechanism cost is about one 30th of the overall robot cost. In that sense, the reduction of 20 to 25% of the undesired force magnitude resulting from the installation of the device brings a worthy benefit.

Current work consists of fabricating better quality fixations, exhibiting less friction, to run a new evaluation under better experimental conditions.

ACKNOWLEDGMENTS

This work was supported in part by the A.N.R. (Agence Nationale de la Recherche) with the projet BRAHMA (BioRobotics for Assisting Human Manipulation) PSIROB 2006.

APPENDIX

Demonstration of Proposition 1

1) Conditions (3) are sufficient: $[(3) \Rightarrow (2)]$.

We here suppose that conditions (3) are verified.

Because in \mathbf{S}_n , \mathcal{R}_{i-1} is connected on one side to \mathcal{R}_0 through \mathbf{S}_{i-1} and on the other side to \mathcal{R}_i through \mathbf{R}_i (see Fig. 3), one has:

$$\forall i \in \{1 \dots n\}, \quad \mathbf{S}_n T_{i-1} = \mathbf{S}_{i-1} T_{i-1} \cap [\mathbf{T}_{\mathbf{R}_i} + \mathbf{S}_n T_i] \quad , \quad (11)$$

which is a recursive relationship for $\mathbf{S}_n T_i$. Recalling that, by assumption, $\mathbf{S}_n T_{\mathbf{S}_n} = \{0\}$ (condition 3c) and $T_{\mathbf{S}_{i-1}} \cap \mathbf{T}_{\mathbf{R}_i} = \{0\}$ (condition 3b), this recursive law trivially leads to (2a).

Furthermore, the kinemato-static duality principle applied to the loop $(\mathcal{R}_0 \rightarrow \mathcal{R}_{i-1} \rightarrow \mathcal{R}_i \rightarrow \mathcal{R}_0)$ in Fig. 3 writes:

$$\forall i \in \{1 \dots n\}, \quad \dim(\mathbf{S}_i W_{\mathbf{L}_i \rightarrow 0}) + \dim(T_{\mathbf{S}_{i-1}} + \mathbf{T}_{\mathbf{R}_i} + \mathbf{T}_{\mathbf{L}_i}) = 6 \quad . \quad (12)$$

Thanks to condition (3a), this leads to:

$$\forall i \in \{1 \dots n\}, \quad \mathbf{S}_i W_{\mathbf{L}_i \rightarrow 0} = \{0\} \quad . \quad (13)$$

Considering again the system \mathbf{S}_i depicted in Fig. 3, and recalling that \mathbf{L}_i and \mathbf{R}_i are serial chains, one has, $\forall i \in \{1 \dots n\}$:

$$\mathbf{S}_i W_{\mathbf{L}_i \rightarrow 0} = \mathbf{S}_i W_{\mathbf{L}_i \rightarrow i} = \mathbf{S}_i W_{\mathbf{R}_i \rightarrow i} = \mathbf{S}_i W_{\mathbf{R}_i \rightarrow i-1} = \{0\} \quad . \quad (14)$$

Therefore, statically speaking, the multi-loop system \mathbf{S}_{i-1} is in the same state when included in \mathbf{S}_i than when isolated from the rest of the mechanism.

$$\forall i \in \{2 \dots n\}, \quad \mathbf{S}_i W_{\mathbf{L}_{i-1} \rightarrow 0} = \mathbf{S}_{i-1} W_{\mathbf{L}_{i-1} \rightarrow 0} \quad ,$$

which, together with (13) recursively leads to condition (2b).

2) Conditions (3) are necessary : $[(3) \Rightarrow (2)]$.

Firstly, if condition (3c) is not verified, then $\mathbf{S}_n T_n = T_{\mathbf{S}_n} \neq \{0\}$. In this case, (2a) is not satisfied.

Secondly, if (3b) is not verified, then $\exists i, (T_{\mathbf{R}_i} \cap T_{\mathbf{S}_{i-1}}) \neq \{0\}$. Thanks to Eq. (11), this leads to:

$$\exists i \in \{1 \dots n\}, \quad \mathbf{S}_n T_{i-1} \neq \{0\} \quad , \quad (15)$$

which directly contradicts (2a).

Thirdly, if (3a) is not verified, i.e.:

$$\exists i, \quad \dim(T_{\mathbf{S}_{i-1}} + \mathbf{T}_{\mathbf{R}_i} + \mathbf{T}_{\mathbf{L}_i}) \leq 6 \quad , \quad (16)$$

then $\exists i, \mathbf{S}_i W_{\mathbf{L}_{i-0}} \neq \{0\}$, meaning that \mathbf{S}_i taken isolate is hyperstatic. Obviously, adding the rest of the mechanism to build \mathbf{S}_n , which consists of adding a parallel branch to \mathbf{S}_i between \mathcal{R}_0 and \mathcal{R}_i will not decrease the degree of hyperstaticity. Therefore $\exists i, \mathbf{S}_n W_{\mathbf{L}_{i-0}} \neq \{0\}$, which contradicts condition (2b).

REFERENCES

- [1] Jose L. Pons. *Wearable Robots: Biomechatronic Exoskeletons*. 2008.
- [2] Scott SH and Winter DA. Biomechanical model of the human foot: kinematics and kinetics during the stance phase of walking. *J Biomech.*, 21993.
- [3] Van der helm, Veeger, and Pronk HG. M. Geometry parameters for musculoskeletal modelling of the shoulder system. *Journal of biomechanics*, June 1992.
- [4] A. Schiele and F.C.T. van der Helm. Kinematic design to improve ergonomics in human machine interaction. *Neural Systems and Rehabilitation Engineering, IEEE Transactions on*, Dec. 2006.
- [5] V. Hayward D. Cai, P. Bidaud and F. Gosselin. Design of self-adjusting orthoses for rehabilitation. *Proceedings of the 14th IASTED International Conference Robotics and Applications*, Nov. 2009.
- [6] A. Schiele. An explicit model to predict and interpret constraint force creation in phri with exoskeletons. *Robotics and Automation, 2008. ICRA 2008. IEEE International Conference on*, pages 1324–1330, May 2008.
- [7] L W Lamoreux. Kinematic measurements in the study of human walking. *Bulletin of Prosthetics Research*, 10(15):3–84, 1971. PMID: 5131748.
- [8] KL Markolf, JS Mensch, and HC Amstutz. Stiffness and laxity of the knee—the contributions of the supporting structures. a quantitative in vitro study. *J Bone Joint Surg Am*, 58(5):583–594, 1976.
- [9] C. Diez-Martinez, J. Rico, J. Cervantes-Sanchez, and J. Gallardo. *Mobility and connectivity in multiloop linkages*, pages 455–464. 2006.
- [10] Stokdijk M.[1], Meskers C.G.M., Veeger H.E.J., de Boer Y.A., and Rozing P.M. Determination of the optimal elbow axis for evaluation of placement of prostheses. *Clinical Biomechanics*, March 1999.
- [11] K.J. Waldron. The constraint analysis of mechanisms. *Journal of Mechanisms*, pages 101–114, 1966.
- [12] P. Garrec, J.P. Friconneau, Y. Measson, and Y. Perrot. Able, an innovative transparent exoskeleton for the upper-limb. *Intelligent Robots and Systems, 2008. IROS 2008. IEEE/RSJ International Conference on*, pages 1483–1488, Sept. 2008.
- [13] Garrec. P. French patent: Transmission vis, ecrou et cable attache a la vis - fr0101630, 2000 (eur 01938347.0-2421 and us 10/296,740 (screw and nut transmission and cable). 2000.
- [14] N. Jarrasse, J. Paik, V. Pasqui, and G. Morel. How can human motion prediction increase transparency? In *Proceedings of IEEE Int Conference on Robotics and Automation*, May 2008.
- [15] N. Jarrasse and G. Morel. A methodology to design kinematics of fixations between an orthosis and a human member. *IEEE/ASME International Conference on Advanced Intelligent Mechatronics*, Jul. 2009.